https://doi.org/10.29227/IM-2025-02-18 Received: 14 Jun 2025, Accepted: 20 Aug 2025, Published: 20 Oct 2025

Features of Gravity Anomalies and Their Oil-Gas Geological Significance in the Cuu Long Basin

TRAN Tuan Duong[1,3,*], TRAN Tuan Dung[1,2], NGUYEN Quang Minh[1], TRAN Trong Lap[1], NGUYEN Thi Nhan[1]

[1] Institute of Earth Sciences, Vietnam Academy of Science and Technology, Hanoi, Vietnam
[2] Graduate University of Science and Technology, Vietnam Academy of Science and Technology, Hanoi, Vietnam
[3] Hanoi University of Mining and Geology, Hanoi, Vietnam
[*] *Corresponding email: ttduong.humg@gmail.com*

Abstract: *This study uses data from the global satellite gravity model SDUST2021GRA and associated processing algorithms (upward continuation and tilt angle of the horizontal gradient) in delineating structural features and hydrocarbon distribution in the Cuu Long Basin (CLB). The gravity anomalies in the CLB are characterized by blocky development in the Northeast-Southwest (NE-SW) and North-South (N-S) direction. According to the changes in amplitudes, the regional gravity anomalies can be classified into four distinct zones. Analysis of gravity data in the CLB indicates that: three main sets of faults are developed in the region, namely, the NE-SW, N-S and NW-ES trending faults. NE-SW trending faults are distributed in a wide range, and they are main faults in the region. They are followed by N-S trending faults, while there are a small number of nearly NW-ES trending faults. Large-scale faults are mainly margin controlling faults for the boundary of the basin and uplifts. Through analysis of gravity anomaly characteristics, combined with location of oil/gas fields, the results show that oil/gas fields in the CLB are mainly located within zones of negative residual gravity anomalies. This approach provides a cost-effective tool for preliminary hydrocarbon exploration and structural evaluation in offshore basins.*

Keywords: *SDUST2021GRA, Upward continuation, Tilt angle of the horizontal gradient, fault systems, Cuu Long basin*

1. Introduction

The CLB is a prolific oil/gas basin situated offshore from the southeastern coast of Vietnam (Fig. 1). It is located between the Vietnamese mainland and the Nam Con Son Basin at the southwestern end of the East Viet Nam Sea. The CLB is a hydrocarbon basin located offshore southern Vietnam in the East Viet Nam Sea. Covering approximately 40.000 km², it is one of Vietnam's most significant petroleum basins, hosting major oil fields such as Bach Ho, Rang Dong, and Ruby.

The CLB is a tectonic structure located offshore southern Vietnam, near the Mekong Delta. The basin extends in a northeasterly direction parallel to the coastline and coastal structures of the Dalat volcano-plutonic zone adjacent to the basin from the northwest. In the southeast, the basin is bounded by the Con Son uplift (Tran Tuan Dung et al., 2024*)*.

The basin formed due to extensional tectonics associated with the opening of the East Viet Nam Sea, influenced by the collision of the Indian and Eurasian plates (*Tapponnier et al., 1982*). Initial rifting in the CLB began in the Eocene–early Oligocene, followed by the uplift and rotation of the crustal blocks at the onset of drifting in the southwestern East Viet Nam Sea. The initial rifting phase is characterized by rapid subsidence and infilling; various alluvial/fluvial/lacustrine processes were involved in the synrift sedimentation. The erosion of the uplifted blocks in the late Oligocene marked the transition from rifting to regional subsidence in the CLB. The postrift unit in the CLB is characterized by a deepeningupward succession, grading upward from nonmarine to paralic or shelf sediments (Lee et al., 2001).

https://doi.org/10.29227/IM-2025-02-18 Received: 14 Jun 2025, Accepted: 20 Aug 2025, Published: 20 Oct 2025

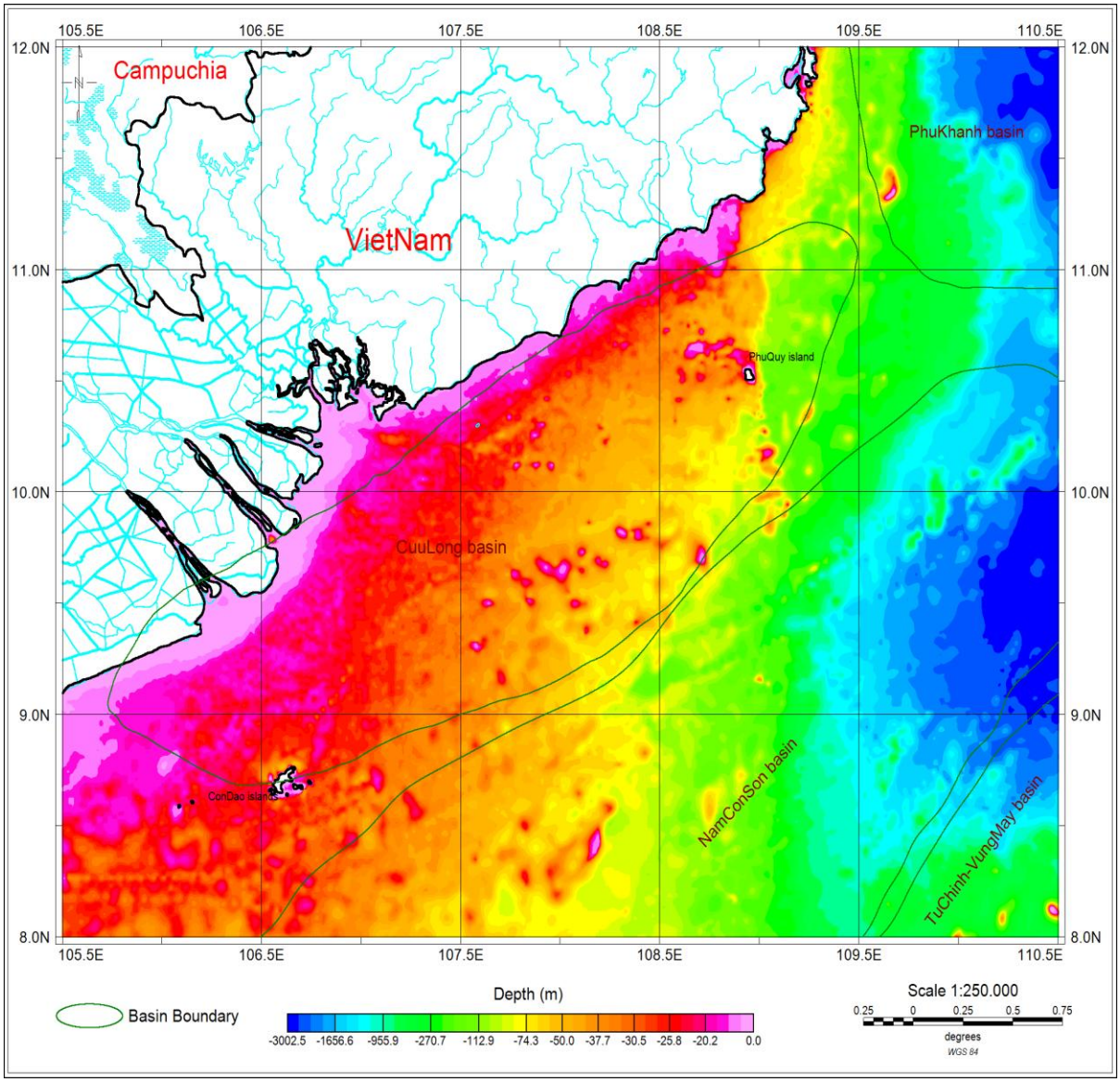

Fig. 1. Location of study area (Cuu Long basin)

A brief description of the basement and overlying sequences follows (William J. Schmidt et al., 2019):

- The basement is made up primarily of intrusive granitoids ranging in age from Middle Jurassic to Latest Cretaceous (Bao et al., 2001) with minor amounts of metamorphic host rocks. Similar granitoids are present onshore in Vietnam (Fyhn et al., 2010; Shellnutt et al., 2013).

- The Middle Eocene F sequence (sometimes referred to locally as the G sequence) is the oldest sedimentary sequence in the basin and is only present in the deepest parts of the basin. It consists of coarsegrained sandstone and conglomerate, with minor amounts of finegrained silt and shale. It was deposited in high-energy alluvial and fluvial environments.

https://doi.org/10.29227/IM-2025-02-18 Received: 14 Jun 2025, Accepted: 20 Aug 2025, Published: 20 Oct 2025

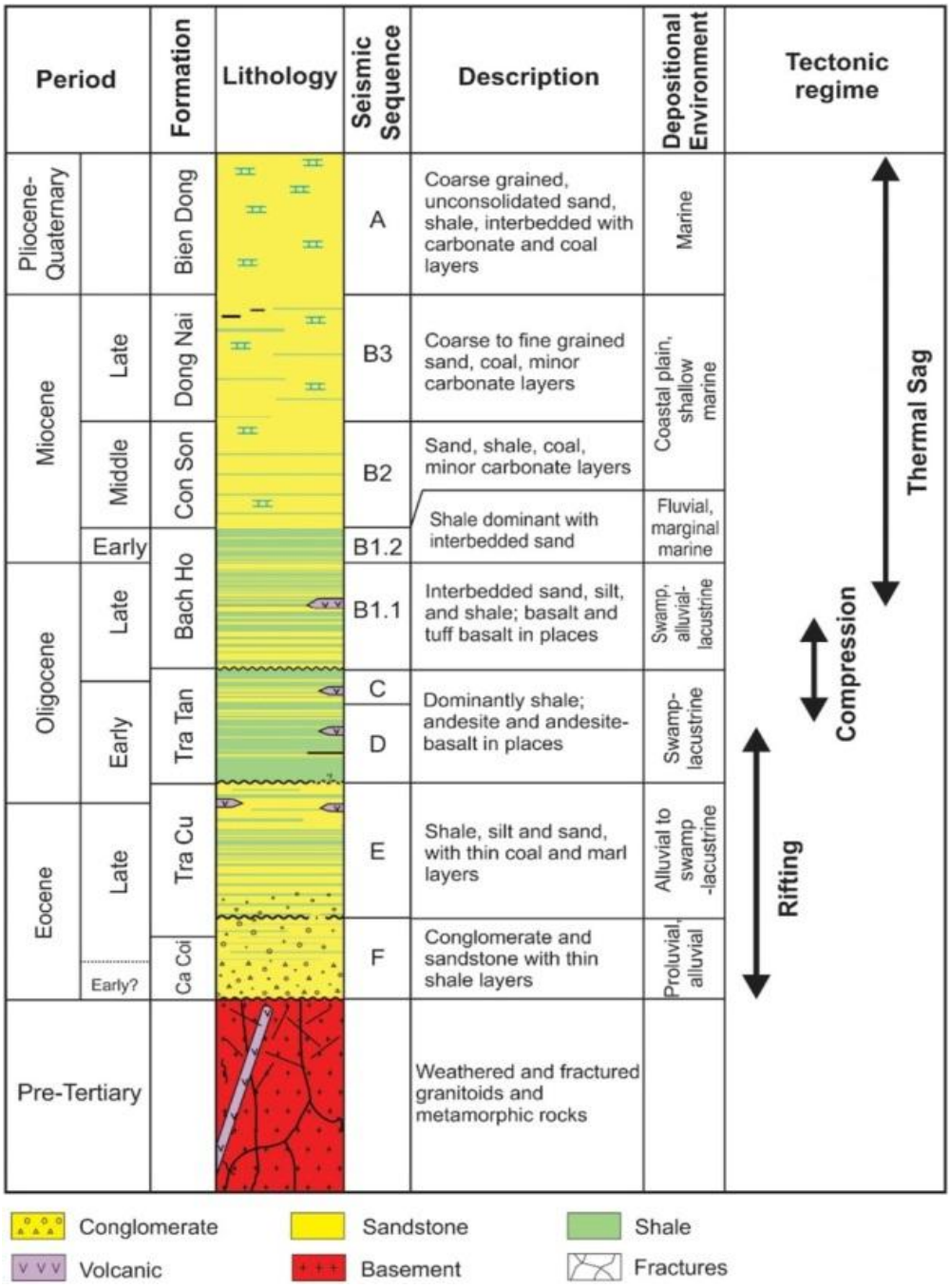

Fig. 2. CLB stratigraphic column with associated depositional environments and tectonic regimes (William et al., 2019)

Gravity method was the first geophysical technique to be used in oil/gas exploration. Despite being eclipsed by seismology, it has continued to be an important and sometimes crucial constraint in a number of exploration areas. In the CLB, these methods have played a crucial role in deciphering the basin's architecture and mapping fault systems, all of which are critical for oil/gas exploration.

2. Data sources and processing technologies

2.1. Sources of gravity data

Global gravity models from satellite altimetry missions have widely contributed to the improvement of the knowledge over the oceans. In the article of Tran Tuan Duong et al., 2024, the accuracy of three global marine gravity models: V32.1GRA, DTU21GRA, and SDUST2021GRA was compared in the Southeast Vietnam sea. The results indicated that the SDUST2021GRA model provided the most accurate results in seafloor depths ranging from 0÷500 meters (Tran Tuan Duong et al., 2024). The global marine gravity anomaly model SDUST2021GRA, has a $1' \times 1'$ grid resolution (https://zenodo.org/records/6668159).

https://doi.org/10.29227/IM-2025-02-18 Received: 14 Jun 2025, Accepted: 20 Aug 2025, Published: 20 Oct 2025

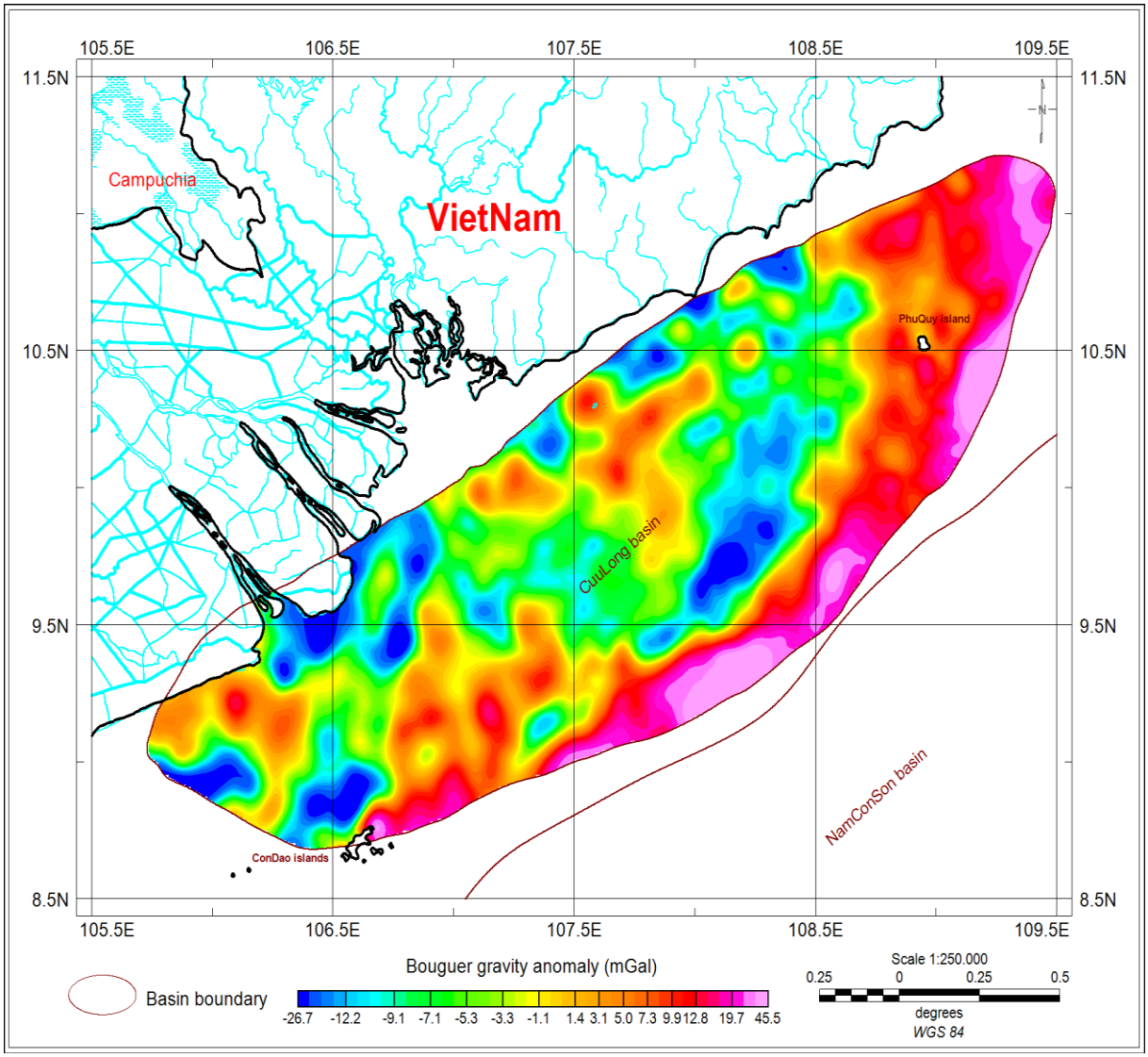

Fig. 3. Map of bouguer gravity anomalies in CLB

Gravity anomaly characteristics: the bouguer map of the CLB exhibits similarities to its corresponding topographic map, with values ranging from −26,7mGal to 45,5mGal (Fig. 3). Areas underlain by denser materials reflect more positive anomalies, while lower density zones generate more negative signatures 0. In the CLB, negative anomalies zones are generally associated with thick sediment accumulations. Conversely, positive anomaly zone, typically coincide with areas of shallower basement or uplifted blocks. The positive low anomaly zone (central area, value anomaly 0 to 5mGal) that sandwiched the negative gravity zone represent the elevated higher-density mantle rocks and thinning of sedimentary deposits.

2.2. Processing technologies

2.2.1. Separation of gravity anomalies:

Upward continuation is a widely used technique for isolating regional gravity anomalies caused by deep sources from the original anomaly data. In order to identify the deep and shallow gravity anomalies and structural characteristics of the study area, the author used the upward continuation method to separate anomalies (Gupta & Ramani, 1980; Jacobsen, 1987). In order to select an appropriate upward extension height, the author extended the gravity anomalies upward at different heights such as 5km, 10km, 15km and 20km (Fig. 4). Since deep and large bodies produced long-wavelength and broad anomaly, upward continuation was applied to smooth out near-surface effects.

https://doi.org/10.29227/IM-2025-02-18 Received: 14 Jun 2025, Accepted: 20 Aug 2025, Published: 20 Oct 2025

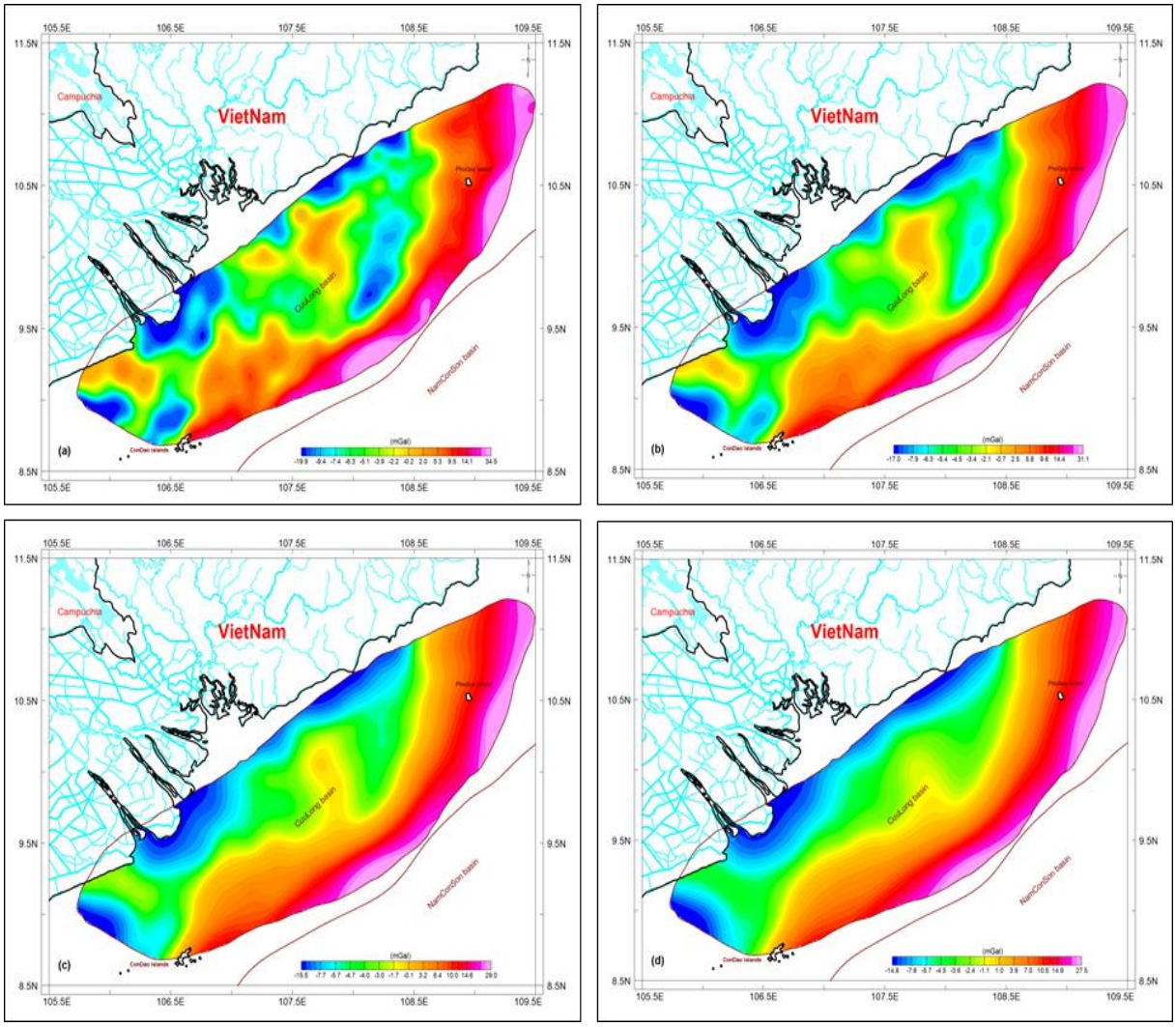

Fig. 4. The anomaly maps of bouguer gravity anomaly after upward continuation at different heights: (a) 5km, (b) 10km, (c) 15km, (d) 20km

The comparison between the 15 km upward continued gravity anomaly (Fig. 4c) and the bouguer gravity anomaly (Fig. 3) shows that the small local anomalies are largely eliminated, and the anomaly becomes smoother, emphasizing deep gravity features. Beyond 15 km, further upward continuation causes minimal change in the overall anomaly patterns. Therefore, the anomalies upward continued to 15 km were selected to represent the regional gravity fields in the study area.

After determining the regional gravity anomalies, the residual gravity anomaly (Fig. 5) was obtained by subtracting the regional gravity anomaly (Fig. 4c) from the bouguer gravity anomaly (Fig. 3).

In Fig. 5, illustrates the residual gravity anomaly maps of the study area. The maps show that the residual anomalies are characterized by complex, alternating high and low anomaly patterns, with evident zonality across the region. Based on the characteristics of residual gravity anomalies, the research region can be partitioned into four anomaly zones: (1): residual gravity anomalies that are more pronounced, trending mostly E-W; (2): residual gravity anomalies that are generally N-S trending; (3): the anormal values of the residual gravity in the zone (3) is an obvious high–value belt in the north and west, and the interior is arranged alternately with local low-value in the NE-SW direction (area bordering zone (4)); (4): residual gravity anomalies exhibit an NE–SW orientation.

https://doi.org/10.29227/IM-2025-02-18 Received: 14 Jun 2025, Accepted: 20 Aug 2025, Published: 20 Oct 2025

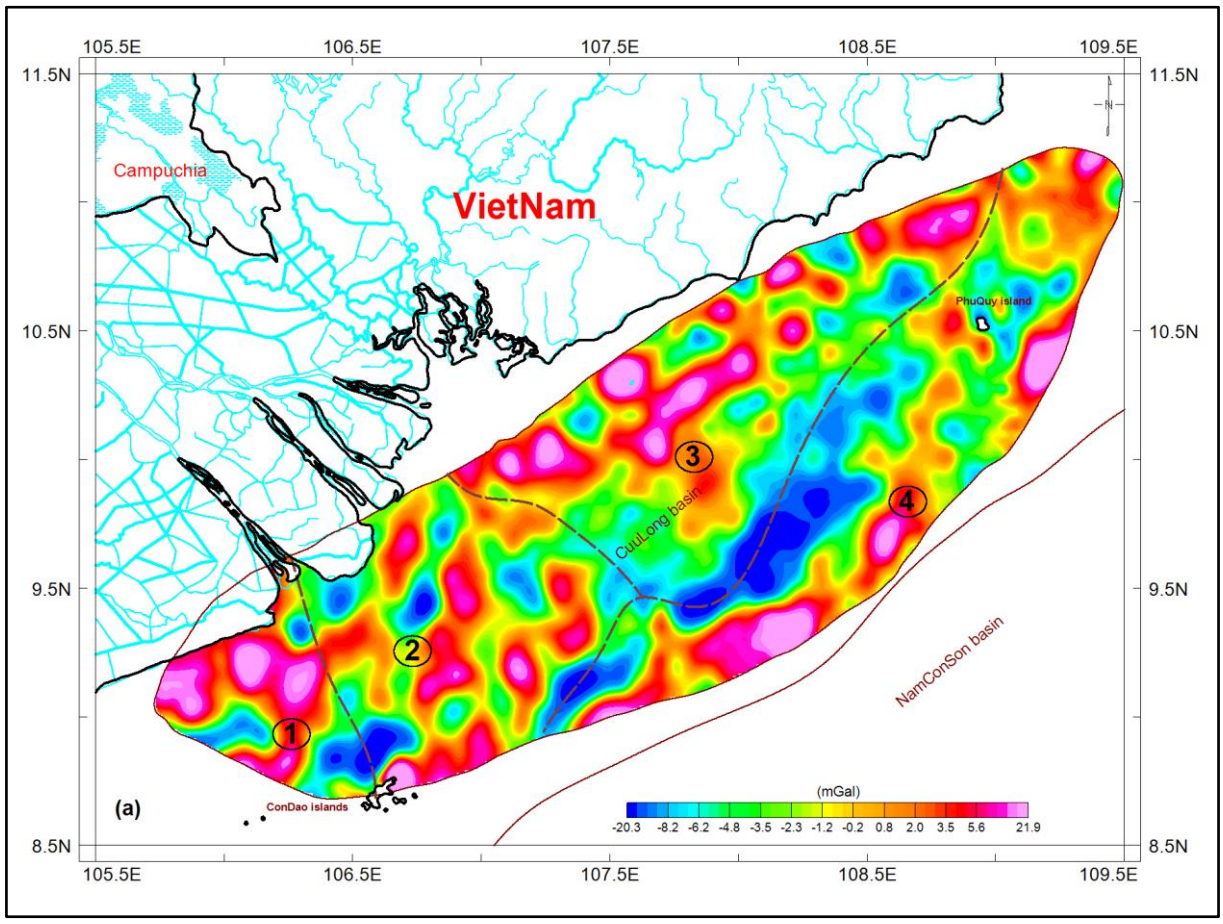

Fig. 5. Map of residual gravity anomalies

2.2.2. Identification of fault systems using gravity data

The tilt angle of the horizontal gradient method (TAHG) is an edge detection method based on total horizontal derivative (THDR) enhancement of gravity anomalies. The main attributes of this method are to provide maximal amplitudes on the source edges and equalize signals from shallow and deep sources (Blakely et al., 1986). The TAHG is obtained by taking the arctangent of the vertical derivative of the THDR, divided by the modulus of the THDR (Ferreira et al., 2013; Tran Tuan Dung et al., 2021; Tran Tuan Duong et al., 2020):

$$TAHG = tan^{-1}\frac{\frac{\partial THDR}{\partial z}}{\sqrt{\left(\frac{\partial THDR}{\partial x}\right)^2 + \left(\frac{\partial THDR}{\partial y}\right)^2}}$$

where:

- $\Delta g(x,y)$ is the gravity anomalies;
- *THDR* is the total horizontal derivative is a prevalent edge-detection filter, as given by (*Cooper et al., 2008*);

$$THDR = \sqrt{\left(\frac{\partial \Delta g(x,y)}{\partial x}\right)^2 + \left(\frac{\partial \Delta g(x,y)}{\partial y}\right)^2}$$

$\frac{\partial \Delta g(x,y)}{\partial x}, \frac{\partial \Delta g(x,y)}{\partial y}$ are first order derivatives of gravity anomaly field in the x, y directions. Due to the characteristics of the arctangent, the *TAHG* transform range is from $\frac{-\pi}{2}$ to $\frac{+\pi}{2}$.

Each grid intersection $TAHG(THDR)_{i,j}$ (except the marginal rows and columns) is compared with its eight nearest neighbors in four directions (along the row, column, and diagonals) to see if a maximum is present (Fig. 6). This comparison tests the following inequalities:

$$TAHG(THDR)_{i-1,j} < TAHG(THDR)_{i,j} > TAHG(THDR)_{i+1,j}$$

$$TAHG(THDR)_{i,j-1} < TAHG(THDR)_{i,j} > TAHG(THDR)_{i,j+1}$$
$$TAHG(THDR)_{i,j-1} < TAHG(THDR)_{i,j} > TAHG(THDR)_{i-1,j-1}$$
$$TAHG(THDR)_{i-1,j-1} < TAHG(THDR)_{i,j} > TAHG(THDR)_{i+1,j+1}$$

A counter N is increased by one for each satisfied inequality. Hence, N ranges from 0 to 4 and provides a measure of the "quality" of the maximum; we shall refer to the parameter N as the "significance level" of the maximum. In this paper, Choosing N ≥ 2 (*Tran Tuan Duong et al., 2020, Tran Tuan Duong et al., 2023*), then the position as well as the maximum value of $TAHG(THDR)_{i,j}$ will be determined:

$$x_{max} = \frac{-bd}{2a}$$

where:

$$a = \frac{1}{2}(TAHG(THDR)_{i-1,j} - 2TAHG(THDR)_{i,j} + TAHG(THDR)_{i+1,j})$$
$$b = \frac{1}{2}(TAHG(THDR)_{i+1,j} - TAHG(THDR)_{i-1,j})$$

d is the distance between grid intersections. The value of the horizontal gradient at x_{max} is given by:

$$TAHG(THDR)_{max} = ax_{max}^2 + bx_{max} + TAHG(THDR)_{i,j}$$

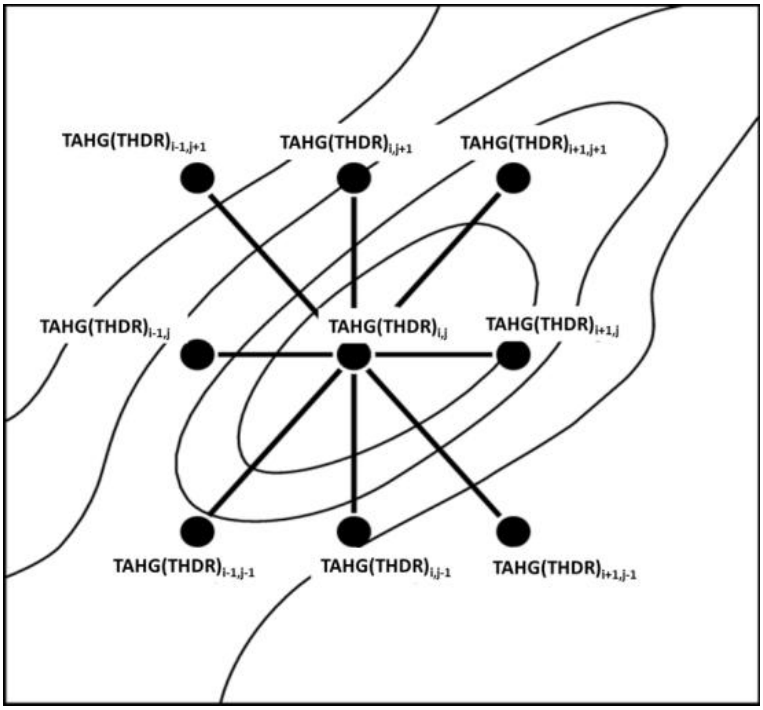

Fig. 6. Location of grid intersections used to test for a maximum near $TAHG(THDR)_{i,j}$, Curved lines represent contours of horizontal gradient values of gravity anomalies

If more than one inequality is satisfied, the largest $TAHG(THDR)_{max}$ and its corresponding x_{max} are chosen as the appropriate maxima for that grid intersection (*Blakely et al., 1986*).

By analyzing and connecting the locations and magnitudes of the TAHG points in a suitable approach, the spatial distribution of the faults system is determined and shown in the Fig. *7*. As can be seen in the Fig. *7*, two main sets of faults are developed in the region, namely: the NE-SW trending and nearly N-S trending faults. NE-SW trending faults are distributed in a wide range, and they are main faults in the region. They are followed by N-S trending faults, while there are a small number of nearly E-W trending faults. Large-scale faults are mainly margin controlling faults for the boundary of the basin and uplifts.

As shown in Figure 7, the oil/gas bearing structures are located in the center of the CLB, situated between two NE–SW oriented fault zones and at fault intersections, particularly between NE–SW and N–S faults as well as between NE–SW and NW–SE faults.

https://doi.org/10.29227/IM-2025-02-18 Received: 14 Jun 2025, Accepted: 20 Aug 2025, Published: 20 Oct 2025

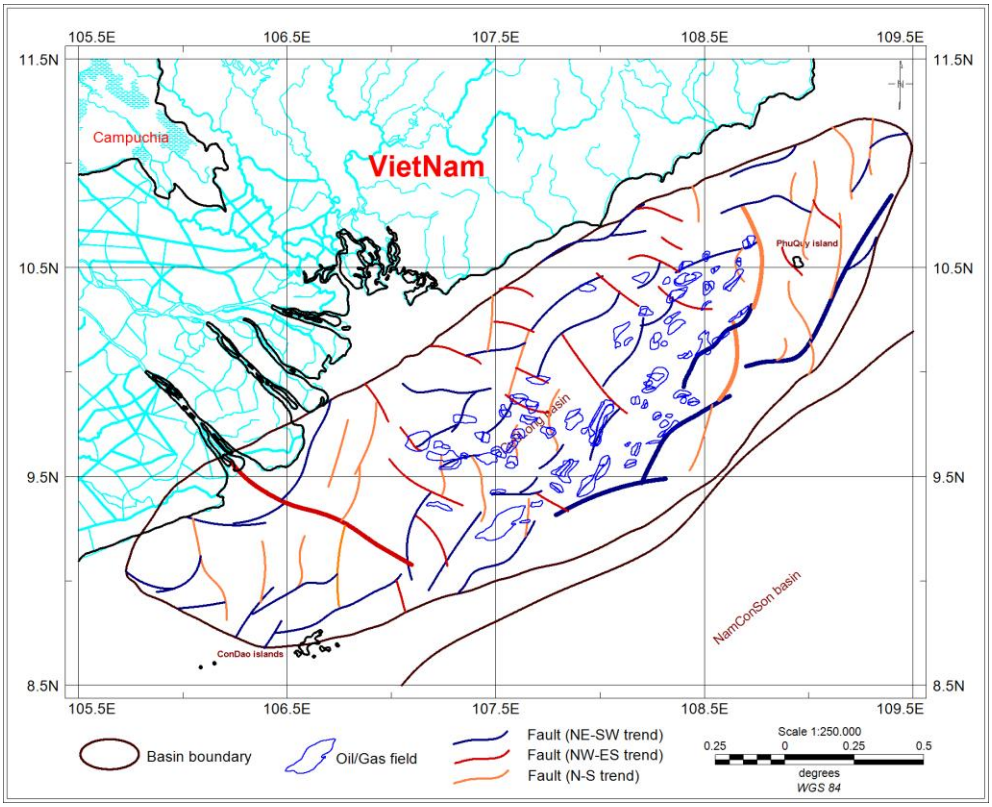

Fig. 7. Fault distribution map of the CLB derived from the interpretation of gravity data (location of oil/gas fields is quoted from the study of Tran Tuan Dung et al., 2024)

3. Prediction of potential oil/gas areas

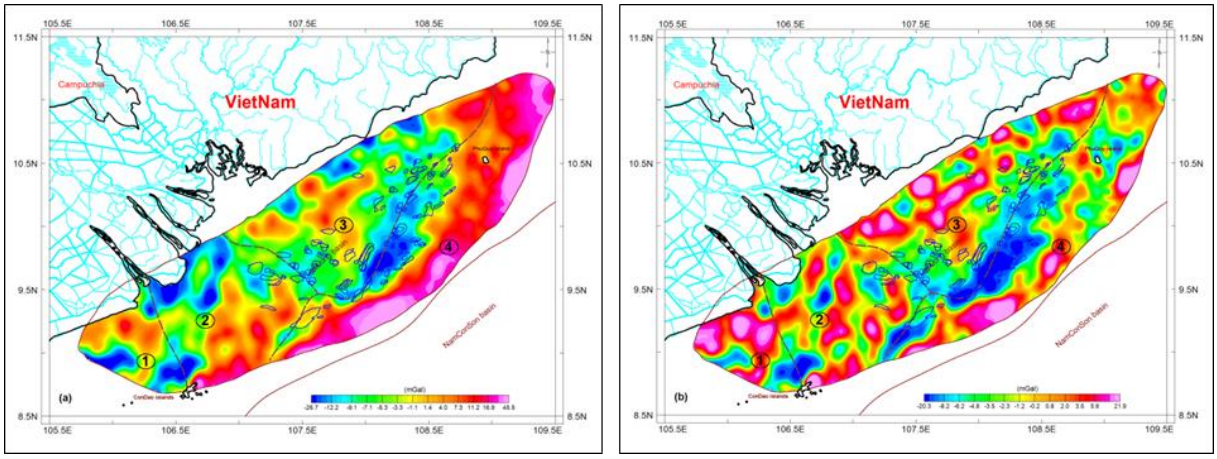

Fig. 8. a) gravity anomalies; b) residual gravity anomalies

In the Fig. ***8***a, the oil/gas fields are primarily located in areas characterized by negative gravity anomalies. Negative bouguer gravity anomalies typically indicate regions with substantial sediment thickness or fracture zones filled with sedimentary material. In the CLB, since the late Oligocene, the transition from the post-rift phase to a period of slow and stable subsidence (*Lee et al., 2001*), with minimal tectonic disturbance, has favored the preservation of deeper traps, allowing them to retain hydrocarbons without significant remigration or leakage.

Similarly, in Fig. 8b, the major oil/gas fields are situated in areas with negative residual gravity anomalies. Such anomalies often correspond to local zones where the sediment layer is thicker and less density than the surrounding rocks, providing favorable conditions for hydrocarbon accumulation.

The integrated interpretation of bouguer and residual gravity anomaly maps (Fig. 8), combined with the distribution of identified fault systems (Fig. 7), enables the delineation of promising oil/gas fields in the CLB. The analysis indicates that most potential oil/gas fields are located in areas where: the residual gravity anomalies exhibit negative values; structures are located within zones of negative gravity

anomalies; situated in proximity to NE–SW–trending faults. These results are consistent with interpretations derived from seismic and well data.

4. Conclusions

Analysis of gravity data identified the main tectonic features in the CLB, mainly NE–SW and N–S trending faults consistent with previous interpretations based on seismic and well data. This consistency validates the reliability of satellite gravity data in capturing large-scale basin structural. The analysis confirms that most oil/gas fields in the CLB are located within zones of negative residual gravity anomalies.

The results of this study demonstrate that satellite gravity data, when processed with appropriate algorithms, can serve as an effective and cost-effective tool for preliminary oil/gas fields. This approach is particularly valuable in offshore or frontier areas where seismic coverage is limited.

Overall, the research highlights the methodological potential of satellite gravity models to complement traditional geophysical data and to provide rapid insights into basin structure and hydrocarbon prospectivity.

Acknowledgments

The authors wish to thank the Vietnam National Project ĐTĐLCN.07/23 and VAST's Projects ĐLTE00.04/24-25 for supporting the necessary conditions to complete this research.

References

Bao, Nguyen Xuan; Van Binh, Nguyen; Long, Pham Huy; Van Long, Trinh; Van Linh, Do; et al., (2001). Structure and Metallogeny of Vietnam.

Blakely, R.J.; Simpson, R.W. (1986). Approximating edges of source bodies from magnetic or gravity anomalies. Geophysics, 51, 1494-1498.

Eze, O.E.; Okiwelu, A.A.; Ekwok, S.E.; Abdelrahman, K.; Alzahrani, H.; Ben, U.C.; Ibrahim, A.; Akpa, C.; Andráš, P.; Ugar, S.I.; Eldosouky, A.M. (2024) Delineation of deep-seated crustal structures from magnetic data in the southeastern part of the Niger Delta basin, Nigeria. Front. Earth Sci. 12:1439199. https://doi.org/10.3389/feart.2024.1439199.

Frifita, N.; Arfaoui, M.; Zargouni, F. (2016). Relationship between surface and subsurface structures of the northern Atlas foreland of Tunisia deduced from regional gravity analysis. Journal of Geophysics and Engineering. 13. 634-645. https://doi.org/10.1088/1742-2132/13/4/634.

Fyhn, M.B.W.; Pedersen, S.A.S.; Boldreel, L.O.; Nielsen, L.H.; Green, P.F.; Dien, P.T.; Frei, D. (2010). Paleocene-early Eocene inversion of the Phuquoc-Kampot Som Basin: SE Asian deformation associated with the suturing of Luconia. J. Geol. Soc. 167 (2), 281–295. https://doi.org/10.1144/0016-76492009-039.

Gupta, V.; Ramani, N. (1980). Some aspects of regional-residual separation of gravity anomalies in a Precambrian, Geophysics, 45, 1412−1426.

Jacobsen, B. (1987). A case for upward continuation as a standard separation filter for potential-field 16 maps, Geophysics, 52, 1138−1148.

Lee, G.H.; Lee, K.; Watkins, J.S. (2001). Geologic evolution of the Cuu Long and Nam Con Son basins, offshore southern Vietnam, South China Sea: American Association of Petroleum Geologists Bulletin, 85, 1055−1082.

Lowrie, W.; Fichtner, A. (2019) Fundamentals of Geophysics. Cambridge University Press.

Shellnutt, J.G.; Lan, C.-Y.; Van Long, T.; Usuki, T.; Yang, H.-J.; Mertzman, S.A.; ... Hsu, W.-Y. (2013). Formation of Cretaceous Cordilleran and post-orogenic granites and their microgranular enclaves from the Dalat zone, southern Vietnam: tectonic implications for the evolution of Southeast Asia. Lithos 182–183, 229–241. https://doi.org/10.1016/j.lithos.2013.09.016.

Tapponnier, P.; Peltzer, G.; Le Dain, A.Y.; Armijo, R. (1982). Propagating extrusion tectonics in Asia: new insights from simple experiments with plasticine. Geology 10, 611–616.

Tran Tuan Dung; Kulinich, R.G.; Nguyen Quang Minh; Nguyen Van Sang; Tran Tuan Duong. (2021). A Study on the Possibility of the Reactivation of the Fault System in the Western Part of the Bien Dong as a Source of Geological Hazards. ISSN 1819-7140, Russian Journal of Pacific Geology, 15, 6, 555–569.

Tran Tuan Dung; Kulinich, R.G.; Tran Tuan Duong; Nguyen Van Sang; Nguyen Quang Minh; Tran

Trong Lap; Nguyen Ba Dai. (2024). Analysis of the Correlation between the Strike Direction of Oil-Gas Accumulations and Fault Systems in the Western South China Sea. ISSN 1819-7140, Russian Journal of Pacific Geology, 2024, 18(6), pp. 732–744. https://doi.org/10.1134/S1819714024700428.

Tran Tuan Duong; Nguyen Quang Minh; Tran Trong Lap. (2024). Evaluation of global marine gravity models using shipborne gravity data in the Southeast Vietnam sea. Proceeding: ERSD 2024, pp 141-149. ISBN: 978-604-76-3040-0.

Tran Tuan Duong; Tran Tuan Dung; Nguyen Ba Dai; Tran Trong Lap; Nguyen Kim Dung; Tran Xuan Loi; Bui Ngoc Quang; Tran Hoang Tam. (2020). Evaluating the effectiveness of total horizontal derivative method and tilt angle of the horizontal gradient method in determining fault structure on the continental shelf and in deep water in the East Sea of Vietnam. Vietnam Journal of Marine Science and Technology, 20(4B), 205–214. https://doi.org/10.15625/1859-3097/15832.

Tran Tuan Duong; Tran Tuan Dung; Nguyen Quang Minh; Tran Trong Lap. (2023). Forecast of submarine landslides related to the reactive probability of the fault system in the southeast vietnam continental shelf and adjacent areas. Proceedings: Geospatial Integrated Technologies for Natural Hazards and Environmental Problems, International Conference GIS-IDEAS 2023, pp 20-28. ISBN: 978-604-357-207-0.

William, J.S.; Bui Huy Hoang; James, W.H.; Vu Trong Hai; Trinh Xuan Cuong; Nguyen Thanh Tung. (2019). Tectonic evolution and regional setting of the Cuu Long Basin, Vietnam**.** Tectonophysics, 757, 36–57. https://doi.org/10.1016/j.tecto.2019.03.001

Zhu, C. (ed.) (2022). SDUST2021GRA: Global marine gravity anomaly model recovered from Ka-band and Ku-band satellite altimeter data, https://doi.org/10.5281/zenodo.6668159.